The Astrophysical Journal Letters, 841:L2 (5pp), 2017 May 20 https://doi.org/10.3847/2041-8213/aa6ffc

Evidence from *K2* for Rapid Rotation in the Descendant of an Intermediate-mass Star

J. J. Hermes[1,7], Steven D. Kawaler[2], A. D. Romero[3], S. O. Kepler[3], P.-E. Tremblay[4], Keaton J. Bell[5], B. H. Dunlap[1], M. H. Montgomery[5], B. T. Gänsicke[4], J. C. Clemens[1], E. Dennihy[1], and S. Redfield[6]
[1] Department of Physics and Astronomy, University of North Carolina, Chapel Hill, NC 27599, USA; jjhermes@unc.edu
[2] Department of Physics and Astronomy, Iowa State University, Ames, IA 50011, USA
[3] Instituto de Física, Universidade Federal do Rio Grande do Sul, Porto Alegre, RS, Brazil
[4] Department of Physics, University of Warwick, Coventry CV4 7AL, UK
[5] Department of Astronomy, University of Texas at Austin, Austin, TX 78712, USA
[6] Wesleyan University Astronomy Department, Van Vleck Observatory, 96 Foss Hill Drive, Middletown, CT 06459, USA
Received 2017 April 12; revised 2017 April 25; accepted 2017 April 27; published 2017 May 15

Abstract

Using patterns in the oscillation frequencies of a white dwarf observed by *K2*, we have measured the fastest rotation rate (1.13 ± 0.02 hr) of any isolated pulsating white dwarf known to date. Balmer-line fits to follow-up spectroscopy from the SOAR telescope show that the star (SDSSJ0837+1856, EPIC 211914185) is a $13{,}590 \pm 340$ K, $0.87 \pm 0.03\,M_{\odot}$ white dwarf. This is the highest mass measured for any pulsating white dwarf with known rotation, suggesting a possible link between high mass and fast rotation. If it is the product of single-star evolution, its progenitor was a roughly $4.0\,M_{\odot}$ main-sequence B star; we know very little about the angular momentum evolution of such intermediate-mass stars. We explore the possibility that this rapidly rotating white dwarf is the byproduct of a binary merger, which we conclude is unlikely given the pulsation periods observed.

Key words: stars: individual (EPIC 211914185) – stars: oscillations (including pulsations) – stars: rotation – white dwarfs

1. Introduction

Thanks to long-baseline monitoring enabled by space missions like *CoRoT* and *Kepler*, we now have deep insight into the angular momentum evolution of low-mass stars (Aerts 2015). Asteroseismology enables the measuring of core and surface rotation rates for numerous 1–3 $M_{\odot}$ stars along the main sequence (e.g., Van Reeth et al. 2016; Ouazzani et al. 2017 and references therein) and along their first ascent up the red giant branch (e.g., Mosser et al. 2012), as well as in core-helium-burning, secondary clump giants (Deheuvels et al. 2015).

As powerful as the *Kepler* seismology has been, it has so far determined internal rotation rates for just a few intermediate-mass stars ($3 < M < 8\,M_{\odot}$) on the main sequence (e.g., Pápics et al. 2017 and references therein). Therefore, we have few constraints on the past or future evolution of angular momentum in Cepheids; rotation can have a significant evolutionary impact on these standard candles (Anderson et al. 2014).

As with all low-mass stars, intermediate-mass stars below roughly $8\,M_{\odot}$ will end their lives as white dwarfs. We can therefore constrain the final stages of angular momentum evolution of intermediate-mass stars by observing white dwarfs. The majority of field white dwarfs have an overall mass narrowly clustered around $0.62\,M_{\odot}$, as determined by fits to the pressure-broadened Balmer lines of hydrogen-atmosphere (DA) white dwarfs (Tremblay et al. 2016). Initial-final mass relations calibrated using white dwarfs in clusters suggest that $0.62\,M_{\odot}$ white dwarfs evolved from roughly $2.2\,M_{\odot}$ main-sequence progenitors (e.g., Williams et al. 2009).

Currently, known white dwarf rotation rates lead to expected rotational broadening well below currently measured upper limits, usually $v \sin i < 10$ km s^{-1} (Berger et al. 2005). Thus, our best insights into the rotation rates of white dwarfs evolving without binary influence come from asteroseismology. To date, the rotation of roughly 20 white dwarfs has been measured from their pulsations, with rotation periods spanning 0.4–2.2 days (Kawaler 2015). All but two have masses less than $0.73\,M_{\odot}$, suggesting that they generally represent the endpoints of $<3.0\,M_{\odot}$ progenitors.

Thanks to its tour of many new fields along the ecliptic, the second life of the *Kepler* space telescope, *K2*, is rapidly increasing the number of white dwarfs with nearly uninterrupted, multi-month light curves suitable for measuring interior rotation rates in these stellar remnants (e.g., Hermes et al. 2017). We present here the discovery of pulsations in a massive white dwarf—likely the descendant of a roughly $4.0\,M_{\odot}$ main-sequence star—which we find to be the most rapidly rotating pulsating white dwarf known to date.

2. Pulsation Periods from *K2*

We targeted the star SDSSJ083702.16+185613.4 (hereafter SDSSJ0837+1856, EPIC 211914185) during *K2* Campaign 5 as part of a search for transits around white dwarfs using the shortest-cadence observations possible (program GO5073). SDSSJ0837+1856 was not observed as part of our GO program to search for pulsations in white dwarfs, as we believed it to be too faint ($K_p = 18.9$ mag). It was selected as a candidate white dwarf from the photometric catalog of Gentile Fusillo et al. (2015), based on its blue colors and relatively high proper motion.

We produced an extracted light curve from the processed target pixel file using the PyKE software package (Still & Barclay 2012), with a fixed aperture of 5 pixels. We removed *K2* motion-induced noise with the KEPSFF task (Vanderburg & Johnson 2014). Our final 74.84 days light curve has 108,454

[7] Hubble Fellow.

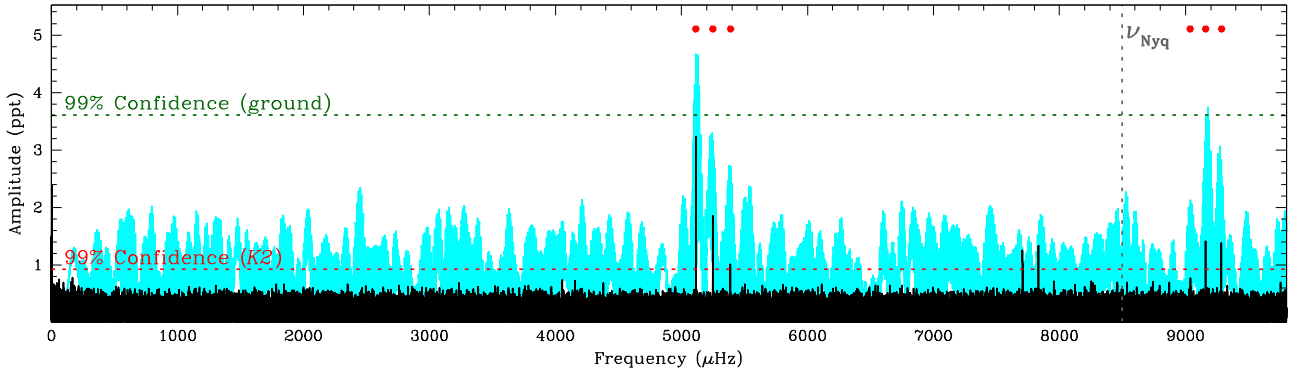

Figure 1. Fourier transform of the *K2* data of SDSSJ0837+1856 (shown in black) showing six frequencies of stellar variability, marked with red dots. A Fourier transform of follow-up ground-based photometry from the 2.1 m Otto Struve telescope at McDonald Observatory and the 4.1 m SOAR telescope, shown in cyan, resolves the Nyquist ambiguity caused by the 58.8 s *K2* short-cadence exposures. The pulsation modes are shown in more detail in Figure 3.

points and a duty cycle of nearly 98.7%, after iteratively clipping all of the points falling $>5\sigma$ from the mean with the VARTOOLS software package (Hartman & Bakos 2016). All of the phases in our light curve are relative to the mid-time of the first exposure: 2457139.6008052 BJD_{TDB}.

We display in Figure 1 a Fourier transform (FT) of our *K2* observations, extending past the Nyquist frequency near 8496 μHz, based on our 58.85 s sampling rate. Our FTs have all been oversampled by a factor of 20; all instrumental harmonics of the long-cadence sampling rate (see Gilliland et al. 2010) have been fit and removed. We show the confidence threshold of the FT determined by simulating 10,000 light curves, wherein we kept the time sampling but randomly shuffled the fluxes, as outlined in Hermes et al. (2015). Of these synthetic FTs, 99.0% do not have a peak exceeding 0.92 ppt (where 1 ppt = 0.1%), which we adopt as our 99% confidence threshold (shown as a red dotted line in Figure 1). This is close to five times the average amplitude of the entire FT: $5\langle A\rangle = 0.98$ ppt.

Notably, two significant peaks in the FT fall within 800 μHz of the Nyquist frequency; in fact, both peaks mirrored above the Nyquist frequency have more than 5% higher amplitudes than their sub-Nyquist counterparts. To resolve this Nyquist ambiguity we obtained follow-up, time-series photometry at higher cadence over four nights in 2017 January, from both the 2.1 m Otto Struve telescope at McDonald Observatory in West Texas and the 4.1 m SOAR telescope at Cerro Pachón in Chile. All of the observations were obtained using blue-broadband, red-cutoff filters.

Our 2.1 m McDonald data were taken over three nights with the frame-transfer ProEM camera, using 10 s exposures taken through a 3 mm *BG40* filter: on 2017 January 23 (4.8 hr long, variable $\sim$1.″6 seeing, thin clouds), 2017 January 24 (2.4 hr long, variable $\sim$2.″0 seeing, clear skies), and 2017 January 26 (2.0 hr long, variable $\sim$2.″3 seeing, clear skies). In addition, we obtained 2.7 hr of time-series photometry on 2017 January 26 (stable $\sim$1.″8 seeing, clear skies) on the 4.1 m SOAR telescope using the Goodman spectrograph in imaging mode, using 17 s exposures through an *S8612* filter. We began collecting our SOAR light curve 2.6 hr before the McDonald data that night, giving us a two-site duty cycle of more than 16% over 72 hr.

Light curves of the ground-based photometry were extracted with circular aperture photometry and corrected to the Solar System barycenter using WQED (Thompson & Mullally 2013). An FT of the ground-based data is shown in cyan in Figure 1, including the 99% confidence threshold of 3.6 ppt, calculated in the same way as the *K2* data. The ground-based data have two significant peaks: one at 5116.53 $\pm$ 0.30 μHz (4.7 $\pm$ 0.7 ppt) and another at 9177.56 $\pm$ 0.38 μHz (3.7 $\pm$ 0.7 ppt), confirming that the super-Nyquist signals from the *K2* data are in fact those in the star. In both cases, daytime observing gaps have conspired to raise an alias peak to the highest peak in the ground-based data set (the frequency uncertainties quoted are not appropriate estimates of the actual uncertainties due to the presence of aliases).

Table 1
Frequencies Present in SDSSJ0837+1856

ID	Frequency (μHz)	Period (s)	Amplitude (ppt)	Phase (rad/2π)
f_{1a}	5112.5995(41)	195.59522	3.23	0.3312(77)
f_{1b}	5250.6035(72)	**190.45430**	1.85	0.837(13)
			$f_{1b} - f_{1a} = 138.004(11)$ μHz	
f_{1c}	5389.852(13)	185.53384	1.03	0.832(24)
			$f_{1c} - f_{1b} = 139.249(20)$ μHz	
f_{2a}	9037.205(17)	110.65368	0.76	0.921(32)
f_{2b}	9161.6178(94)	**109.15103**	1.40	0.704(18)
			$f_{2b} - f_{2a} = 124.413(27)$ μHz	
f_{2c}	9286.287(10)	107.68566	1.37	0.136(18)
			$f_{2c} - f_{2b} = 124.669(19)$ μHz	

We note that the amplitudes of the ground-based data are at least 20% higher than the *K2* amplitudes. This is partly a result of different limb-darkening in our bluer ground-based filters than in the *Kepler* bandpass (Robinson et al. 1995), as well as flux dilution from a nearby ($<$4.″5, $\Delta K_p \sim 2.8$ mag) galaxy. More significantly, we expect phase-smearing from the 58.85 s exposures to suppress the *K2* amplitudes around f_1 by more than 14% and f_2 by more than 40%.

Informed by our higher-cadence photometry from McDonald and SOAR, we display in Table 1 all six of the pulsation frequencies that we detected in SDSSJ0837+1856, marking in bold the $m = 0$ components. We include one mode—f_{2a}—for which we have slightly relaxed the significance threshold, since it falls where we would expect for a component of a rotationally split multiplet (see Section 4); our synthetic FTs estimate a 13% confidence in f_{2a}. The values in Table 1 have been computed with a simultaneous nonlinear least squares fit for the frequency, amplitude, and phase to the *K2* data using PERIOD04 (Lenz & Breger 2005). The amplitudes have a formal uncertainty of 0.16 ppt. Our period determination is not in the stellar rest frame, but is at high enough precision that it

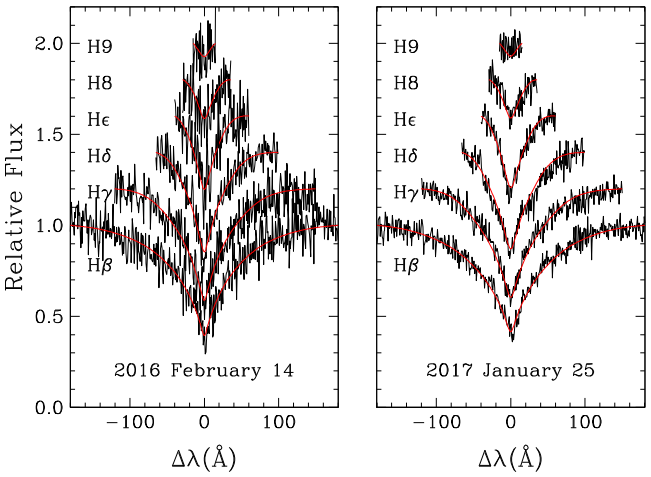

Figure 2. Averaged spectra of 2 × 600 s exposures the night of 2016 February 14 (left) and of 9 × 600 s exposures on 2017 January 25 (right) obtained with the high-throughput Goodman spectrograph on the 4.1 m SOAR telescope. A weighted mean of both fits finds that SDSSJ0837+1856 is a 13,590 ± 340 K, 0.87 ± 0.03 $M_\odot$ white dwarf.

should be corrected for the gravitational redshift and line-of-sight motion of the white dwarf (e.g., Davies et al. 2014).

3. Mass Determination from Spectroscopy

With just two independent pulsation modes at 109.15103 s and 190.45430 s, we have only limited asteroseismic constraint on the properties of SDSSJ0837+1856. Therefore, we obtained low-resolution spectra of as many Balmer lines as possible using the Goodman spectrograph on the 4.1 m SOAR telescope (Clemens et al. 2004). Our setup covers the wavelength range 3600–5200 Å with a dispersion of roughly 0.8 Å pixel^{-1}. We used a 3″ slit, so our spectral resolution is seeing limited, roughly 5 Å in 1.″5 seeing.

We obtained spectra of SDSSJ0837+1856 over two nights with SOAR. On the night of 2016 February 14 we obtained consecutive 2 × 600 s exposures in 1.″4 seeing at an airmass of 1.8, giving us a signal-to-noise ratio (S/N) of 26 per resolution element in the continuum around 4600 Å. Subsequently, we obtained 9 × 600 s exposures on the night of 2017 January 25 in 2.″0 seeing at an airmass of 1.4, yielding S/N = 61.

We optimally extracted all of the spectra (Horne 1986) with the PAMELA software package. We subsequently used MOLLY (Marsh 1989) to wavelength calibrate and apply a heliocentric correction. We flux calibrated the 2016 February spectra with the spectrophotometric standard GD 71, and the 2017 January spectra with Feige 67.

We fit the six Balmer lines Hβ–H9 for each epoch of spectroscopy to pure-hydrogen, 1D model atmospheres for white dwarfs that employ the ML2/α = 0.8 prescription of the mixing-length theory; the models and fitting procedures are described in Tremblay et al. (2011) and were convolved to match the resolution set by the seeing. For both epochs we find atmospheric parameters indicating a relatively hot and massive white dwarf: for 2016 February 14 we find 1D parameters of $T_{\rm eff}$ = 13,010 ± 370 K, $\log g$ = 8.503 ± 0.072, and for 2017 January 25 we find $T_{\rm eff}$ = 14,020 ± 300 K, $\log g$ = 8.412 ± 0.044. We display the Balmer-line fits in Figure 2.

A weighted mean of both epochs yields 1D atmospheric parameters of $T_{\rm eff}$ = 13,620 ± 340 K, $\log g$ = 8.437 ± 0.052. We can correct these for the three-dimensional dependence of convection (Tremblay et al. 2013), which slightly modifies the temperature to 13,590 K and surface gravity to $\log g$ = 8.434.

The 3D-corrected parameters of SDSSJ0837+1856 correspond to a white dwarf mass of 0.87 ± 0.03 $M_\odot$ using the models of Romero et al. (2013). If it evolved in isolation, SDSSJ0837+1856 would have descended from a roughly 4.0 ± 0.5 $M_\odot$ B-star progenitor (Cummings et al. 2016).

4. Asteroseismic Measurement of Rotation

White dwarfs oscillate in non-radial g-modes. In the absence of rotation, pulsations with the same angular degree, ℓ, and radial overtone, n, have the same frequency, independent of the azimuthal order, m. Rotation can lift this m degeneracy and decompose a mode into $2\ell + 1$ components (Unno et al. 1989). Due to the geometric cancellation of high-ℓ modes, we most commonly observe dipole $\ell = 1$ modes in white dwarfs, which separate into triplets of $m = -1$, 0, 1 components.

Thanks to the nearly unblinking, 74-day stare of *K2*, we see clearly that the two main modes of SDSSJ0837+1856 are each composed of nearly symmetrically split triplets, shown in detail in Figure 3. We can use the frequency splittings within these modes to estimate the rotation rate of this massive white dwarf. The weighted mean of the frequency splittings for each mode are δf_1 = 138.626 ± 0.031 μHz and δf_2 = 124.541 ± 0.046 μHz.

To first order, we can connect an identified frequency splitting (δf) to the overall stellar rotation (Ω) by the relation $\delta f = m(1 - C_{n,\ell})\Omega$, where $C_{n,\ell}$ represents the effect of the Coriolis force on the pulsations as formulated by Ledoux (1951). In white dwarfs, $C_{n,\ell}$ is usually close to an asymptotic value of $1/\ell(\ell + 1) = 0.5$ for $\ell = 1$ (e.g., Winget et al. 1991). Some modes of lower radial order (especially $n < 5$) are strongly affected by abrupt chemical transitions in the layering of the white dwarf, which effectively trap modes in different depths of the star. This trapping causes $C_{n,\ell}$ to deviate below the asymptotic value, and is likely why the mean frequency splittings for δf_1 and δf_2 in SDSSJ0837+1856 differ by more than 14 μHz (10%).

With just two independent modes, our models are only weakly constrained by asteroseismology. However, guided by our spectroscopically determined effective temperature and overall mass, we have used the evolutionary sequences described in Romero et al. (2013) to explore model-dependent values for $C_{n,\ell}$. We identify f_1 at 109.151 s as an $\ell = 1$, $n = 1$ mode, and f_2 at 190.454 s as an $\ell = 1$, $n = 2$ mode. The 13, 590 K, 0.87 $M_\odot$ model, with a canonically thick hydrogen-layer mass computed in Romero et al. (2013), predicts $C_{1,1} = 0.495$ and $C_{2,1} = 0.438$ (with mode periods of 98.05 s and 170.78 s, respectively). From these model-based $C_{n,\ell}$ values, each triplet *independently* yields a rotation period of exactly 1.13 hr, from both δf_1 *and* δf_2.

Our uncertainties concerning the rotation rate are dominated by the model uncertainties in computing $C_{n,\ell}$, which consistently predict that the $\ell = 1$, $n = 2$ mode is highly trapped. The most deviant model from Romero et al. (2013) within our spectroscopic uncertainties (13,590 K, 0.85 $M_\odot$) predicts $C_{1,1} = 0.495$ and $C_{2,1} = 0.428$, yielding a rotation period of 1.15 hr using f_2. Therefore, we adopt a rotation period of 1.13 ± 0.02 hr for SDSSJ0837+1856.

Finally, the frequency splittings between prograde ($m = 0$ to $m = +1$) relative to retrograde ($m = -1$ to $m = 0$) components are asymmetric in SDSSJ0837+1856. That is, the $m = 0$

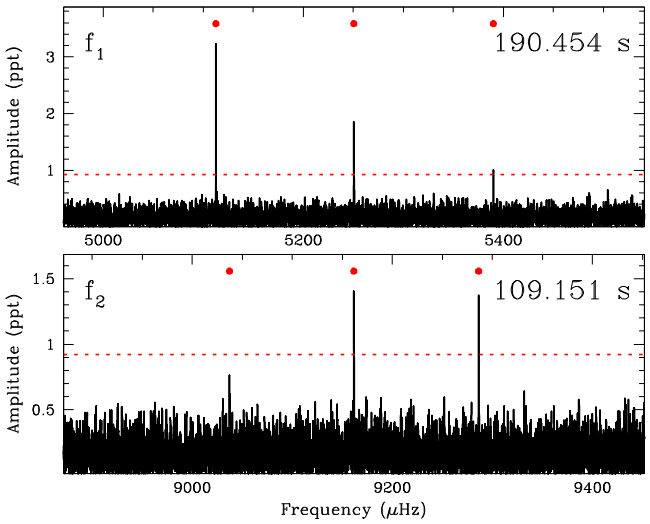

Figure 3. The two main pulsation modes of SDSSJ0837+1856, centered at 190.45430 s and 109.15103 s, are most simply interpreted as triplets of $\ell = 1$ dipole modes. The modes have weighted mean frequency splittings of $\delta f_1 = 138.626$ μHz and $\delta f_2 = 124.541$ μHz, which correspond to a rotation period of 1.13 ± 0.02 hr, faster than any pulsating white dwarf known to date.

component is not exactly centered between the $m = \pm 1$ components. For f_1, the observed $m = 0$ component is displaced to a lower frequency by 0.622 ± 0.043 μHz; for f_2 the value is 0.128 ± 0.073 μHz. The asymmetry is <0.5% and does not significantly affect our inferred rotation rate, but is noteworthy because it likely represents second-order rotation effects, which are expected to be present for such a rapid rotator (Chlebowski 1978). A systematic shift of the $m = 0$ components can also constrain the presence of a magnetic field too weak to detect from Zeeman splitting of spectroscopy (Jones et al. 1989).

5. Discussion and Conclusions

Using *K2*, we have discovered a $T_{\rm eff} = 13{,}590 \pm 340$ K, $0.87 \pm 0.03\,M_\odot$ white dwarf with a rotation period of 1.13 ± 0.02 hr, faster than any known isolated pulsating white dwarf.

To put this rotation in context, we show in Figure 4 asteroseismically deduced rotation rates of apparently isolated white dwarfs with cleanly identified pulsations from the literature, as compiled by Kawaler (2015): GD 154, HL Tau 76, KUV 11370+4222, HS 0507+0434, L19-2, LP 133–144, GD 165, R548, G185-32, G226-29, EC14012-1446, KIC 4552982 (Bell et al. 2015), and KIC 11911480 (DAVs); PG 0122+200, PG 2131+066, NGC 1501, PG 1159-035, and RX J2117.1+3412 (DOVs); and the DBVs KIC 8626021 and PG 0112+104 (Hermes et al. 2017). We have excluded the $0.60\,M_\odot$ white dwarf SDSSJ1136+0409, which rotates at 2.49 ± 0.53 hr but is currently in a 6.9-hr binary with a detached, nearby dM companion; it underwent binary interaction via a common-envelope event (Hermes et al. 2015).

All 20 of the white dwarfs with previously published rotation rates likely evolved in isolation, and span the range of rotation periods between roughly 0.4–2.2 days. All have spectroscopically deduced atmospheric parameters; the sample has a mean mass of $0.64\,M_\odot$ with a standard deviation of $0.08\,M_\odot$, including 3D corrections (Tremblay et al. 2013). This is remarkably similar to the $0.62\,M_\odot$ mean mass of field white dwarfs (Tremblay et al. 2016), suggesting that the majority of isolated, canonical-mass white dwarfs rotate at 0.4–2.2 days.

Figure 4 brings one interesting fact into focus: the three most massive single white dwarfs with rotation measured via asteroseismology are also among the fastest rotators. SDSSJ161218.08+083028.2 (hereafter SDSSJ1612+0830) has significant pulsation periods at 115.17 s and 117.21 s (Castanheira et al. 2013). These pulsation modes are not cleanly identified, but are too close together to be different radial orders. The simplest explanation is that they are components of a single $\ell = 1$ mode split by either 75.6 μHz or 151.2 μHz, indicating a rotation period of roughly 2.0 hr or 1.0 hr, respectively; we mark both solutions in Figure 4. We have refit the SDSS spectrum of SDSSJ1612+0830 using the same models and 3D corrections described in Section 3, and find it has $T_{\rm eff} = 11{,}800 \pm 170$ K, $\log g = 8.281 \pm 0.048$, corresponding to a mass of $0.78 \pm 0.03\,M_\odot$. Other than SDSSJ0837+1856, the only star in Figure 4 that is more massive than SDSSJ1612+0830 is G226-29 ($0.83 \pm 0.03\,M_\odot$), which has a single $\ell = 1$ mode centered at 109.28 s with splittings that indicate 8.9-hr rotation (Kepler et al. 1995).

It is also possible to measure the rotation of white dwarfs from magnetic spots. There are four spotted white dwarfs with rotation rates shorter than 1 hr: RE J0317−853 (12.1 minutes, Vennes et al. 2003), NLTT 12758B (22.6 minutes, Kawka et al. 2017), SDSSJ152934.98+292801.9 (38.1 minutes, Kilic et al. 2015), and G99−47 (58.2 minutes, Bues & Pragal 1989). RE J0317−853 is especially noteworthy since it has a mass inferred from a parallax distance of at least $1.28\,M_\odot$(Külebi et al. 2010); its extremely high magnetic field (>200 MG) suggests it could be the outcome of a binary merger (e.g., García-Berro et al. 2012).

From population synthesis estimates, roughly 7%–23% of all apparently single white dwarfs are expected to be the byproducts of mergers (Toonen et al. 2017). Therefore, it is possible that the white dwarf discovered here, SDSSJ0837+1856, is not the descendant of single-star evolution. Asteroseismology may rule out this scenario. The $0.877\,M_\odot$ model from Romero et al. (2012), highlighted in their Figure 6, shows that it is difficult to observe an $\ell = 1$, $n = 1$, $m = 0$ mode with a pulsation period below 110 s without the white dwarf having a canonically thick hydrogen layer ($\gtrsim 10^{-5}\ M_{\rm H}/M_\star$). For this reason, we prefer a single-star evolutionary model; however, more asteroseismic analysis and modeling is required to definitively rule out a binary-merger origin.

Finally, we note that SDSSJ0837+1856 now supplants HS 1531+7436 as the hottest known isolated DAV; HS 1531+7436 has 3D-corrected atmospheric parameters of $T_{\rm eff} = 13{,}270 \pm 290$ K, $\log g = 8.49 \pm 0.06$, found using the same model atmospheres (Gianninas et al. 2011). However, the best-fit effective temperatures for SDSSJ0837+1856 from spectra taken on two different nights differ by more than 1000 K, a $>2\sigma$ disagreement (the surface gravities are consistent within the uncertainties). Unfortunately, the photometric colors—$(u-g,\ g-r) = (0.36 \pm 0.03,\ -0.21 \pm 0.02)$—do not strongly prefer one solution over the other (Genest-Beaulieu & Bergeron 2014). Given the defining role that SDSSJ0837+1856 may play in setting the blue edge of the DAV instability strip where pulsations driven by hydrogen partial-ionization finally reach observable amplitudes, it is worth more detailed follow-up spectroscopy to obtain a reliably accurate effective temperature.

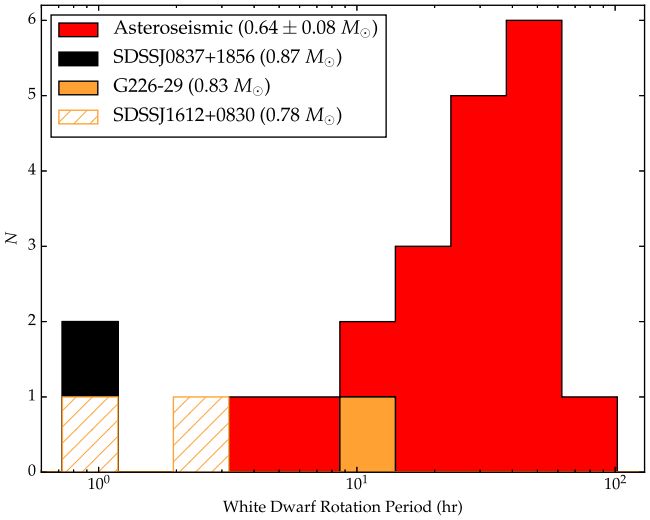

Figure 4. Histogram of rotation rates determined from the asteroseismology of pulsating white dwarfs (marked in red), as collected by Kawaler (2015). SDSSJ0837+1856 (marked in black) is more massive ($0.87 \pm 0.03\ M_\odot$) and rotates faster (1.13 ± 0.02 hr) than any other known pulsating white dwarf. We mark in orange the only two other pulsating white dwarfs $>0.75\ M_\odot$ with rotation estimates. SDSSJ1612+0830 (Castanheira et al. 2013) is not cleanly identified and could rotate at either 1.0 hr or 2.0 hr (see the text).

We acknowledge helpful comments from the anonymous referee, as well as useful discussions with Conny Aerts and Jamie Tayar. Support for this work was provided by NASA through Hubble Fellowship grant #*HST*-HF2-51357.001-A, awarded by the Space Telescope Science Institute, which is operated by the Association of Universities for Research in Astronomy, Incorporated, under NASA contract NAS5-26555; NASA *K2* Cycle 4 Grant NNX17AE92G; NASA *K2* Cycle 2 Grant NNX16AE54G; CNPq and PRONEX-FAPERGS/CNPq (Brazil); NSF grants AST-1413001 and AST-1312983; the European Research Council under the European Union's Seventh Framework Programme (FP/2007-2013)/ERC Grant Agreement n. 320964 (WDTracer); and the European Union's Horizon 2020 Research and Innovation Programme/ERC Grant Agreement n. 677706 (WD3D). Based on observations obtained at the Southern Astrophysical Research (SOAR) telescope, which is a joint project of the Ministério da Ciência, Tecnologia, e Inovação da República Federativa do Brasil, the U.S. National Optical Astronomy Observatory, the University of North Carolina at Chapel Hill, and Michigan State University, as well as data taken at The McDonald Observatory of The University of Texas at Austin.

Facilities: Kepler, SOAR (Goodman), Otto Struve (ProEM).

References

Aerts, C. 2015, AN, 336, 477
Anderson, R. I., Ekström, S., Georgy, C., et al. 2014, A&A, 564, A100
Bell, K. J., Hermes, J. J., Bischoff-Kim, A., et al. 2015, ApJ, 809, 14
Berger, L., Koester, D., Napiwotzki, R., Reid, I. N., & Zuckerman, B. 2005, A&A, 444, 565
Bues, I., & Pragal, M. 1989, in IAU Coll. 114: White Dwarfs, Lecture Notes in Physics, ed. G. Wegner (Berlin: Springer), 329
Castanheira, B. G., Kepler, S. O., Kleinman, S. J., Nitta, A., & Fraga, L. 2013, MNRAS, 430, 50
Chlebowski, T. 1978, AcA, 28, 441
Clemens, J. C., Crain, J. A., & Anderson, R. 2004, Proc. SPIE, 5492, 331
Cummings, J. D., Kalirai, J. S., Tremblay, P.-E., & Ramirez-Ruiz, E. 2016, ApJ, 818, 84
Davies, G. R., Handberg, R., Miglio, A., et al. 2014, MNRAS, 445, L94
Deheuvels, S., Ballot, J., Beck, P. G., et al. 2015, A&A, 580, A96
García-Berro, E., Lorén-Aguilar, P., Aznar-Siguán, G., et al. 2012, ApJ, 749, 25
Genest-Beaulieu, C., & Bergeron, P. 2014, ApJ, 796, 128
Gentile Fusillo, N. P., Gänsicke, B. T., & Greiss, S. 2015, MNRAS, 448, 2260
Gianninas, A., Bergeron, P., & Ruiz, M. T. 2011, ApJ, 743, 138
Gilliland, R. L., Jenkins, J. M., Borucki, W. J., et al. 2010, ApJL, 713, L160
Hartman, J. D., & Bakos, G. Á. 2016, A&C, 17, 1
Hermes, J. J., Gänsicke, B. T., Bischoff-Kim, A., et al. 2015, MNRAS, 451, 1701
Hermes, J. J., Kawaler, S. D., Bischoff-Kim, A., et al. 2017, ApJ, 835, 277
Horne, K. 1986, PASP, 98, 609
Jones, P. W., Hansen, C. J., Pesnell, W. D., & Kawaler, S. D. 1989, ApJ, 336, 403
Kawaler, S. D. 2015, in ASP Conf. Ser. 493, XIX European Workshop on White Dwarfs, ed. P. Dufour, P. Bergeron, & G. Fontaine (San Francisco, CA: ASP), 65
Kawka, A., Briggs, G. P., Vennes, S., et al. 2017, MNRAS, 466, 1127
Kepler, S. O., Giovannini, O., Wood, M. A., et al. 1995, ApJ, 447, 874
Kilic, M., Gianninas, A., Bell, K. J., et al. 2015, ApJL, 814, L31
Külebi, B., Jordan, S., Nelan, E., Bastian, U., & Altmann, M. 2010, A&A, 524, A36
Ledoux, P. 1951, ApJ, 114, 373
Lenz, P., & Breger, M. 2005, CoAst, 146, 53
Marsh, T. R. 1989, PASP, 101, 1032
Mosser, B., Goupil, M. J., Belkacem, K., et al. 2012, A&A, 548, A10
Ouazzani, R.-M., Salmon, S. J. A. J., Antoci, V., et al. 2017, MNRAS, 465, 2294
Pápics, P. I., Tkachenko, A., Van Reeth, T., et al. 2017, A&A, 598, A74
Robinson, E. L., Mailloux, T. M., Zhang, E., et al. 1995, ApJ, 438, 908
Romero, A. D., Córsico, A. H., Althaus, L. G., et al. 2012, MNRAS, 420, 1462
Romero, A. D., Kepler, S. O., Córsico, A. H., Althaus, L. G., & Fraga, L. 2013, ApJ, 779, 58
Still, M., & Barclay, T. 2012, PyKE: Reduction and analysis of Kepler Simple Aperture Photometry Data, Astrophysics Source Code Library, ascl:1208.004
Thompson, S., & Mullally, F. 2013, Wqed: Lightcurve Analysis Suite, Astrophysics Source Code Library, ascl:1304.004
Toonen, S., Hollands, M., Gaensicke, B. T., & Boekholt, T. 2017, arXiv:1703.06893
Tremblay, P.-E., Bergeron, P., & Gianninas, A. 2011, ApJ, 730, 128
Tremblay, P.-E., Cummings, J., Kalirai, J. S., et al. 2016, MNRAS, 461, 2100
Tremblay, P.-E., Ludwig, H.-G., Steffen, M., & Freytag, B. 2013, A&A, 559, A104
Unno, W., Osaki, Y., Ando, H., Saio, H., & Shibahashi, H. 1989, Nonradial Oscillations of Stars (2nd ed.; Tokyo: Univ. Tokyo Press)
Van Reeth, T., Tkachenko, A., & Aerts, C. 2016, A&A, 593, A120
Vanderburg, A., & Johnson, J. A. 2014, PASP, 126, 948
Vennes, S., Schmidt, G. D., Ferrario, L., et al. 2003, ApJ, 593, 1040
Williams, K. A., Bolte, M., & Koester, D. 2009, ApJ, 693, 355
Winget, D. E., Nather, R. E., Clemens, J. C., et al. 1991, ApJ, 378, 326